

AVALANCHE PHOTODIODES FOR HIGH-RESOLUTION PET IMAGING SYSTEMS

R. Bugalho, B. Carriço, C. S. Ferreira, M. Ferreira, R. Moura, C. Ortigão
J. Pinheiro, P. Rodrigues, J. C. Silva, A. Trindade and J. Varela¹

LIP – Lab. de Instrumentação e Física Experimental de Partículas, Avenida Elias Garcia 14, 1000-149 Lisboa, Portugal

¹*also at IST- Instituto Superior Técnico, Av Rovisco Pais, 1049-001 Lisboa, Portugal*

Keywords: Avalanche photodiode, Dark current, Gain, Positron emission mammography, Quality control.

Abstract: A high-resolution Positron Emission Tomography (PET) scanner prototype, named Clear-PEM, was developed by the Portuguese PET Consortium in the framework of the Crystal Clear Collaboration (CCC). This scanner is a PET prototype dedicated for breast cancer imaging mammography, based on a novel readout scheme constituted by fine-pitch scintillator crystals, avalanche photodiodes (APD), low-noise high-gain frontend amplifiers and a reconfigurable FPGA-based electronics readout system. The Clear-PEM scanner is designed to exam both the breast and the auxiliary lymph node areas, aiming at the detection of tumours down to 2 mm in diameter. The prototype has two planar detector heads, each composed of 96 detector modules. Each detector module is composed of a matrix of 32 identical 2x2x20 mm³ LYSO:Ce scintillator crystals, read at both ends by Hamamatsu S8550 APD arrays (4x8) for Depth-of-Interaction (DOI) capability. The APD arrays were characterized through the measurement of gain and dark current as a function of bias voltage, under controlled conditions. A set of 984 APD arrays followed a well defined quality control (QC) protocol, aiming at the rejection of arrays not complying with the defined specifications. From the total of 984, only 1 (0.1%) was rejected, reassuring the trust in these detectors for prototype assembly and future applications.

1 INTRODUCTION

New methods for breast cancer diagnosis are object of heavy research efforts. One such research line relies on the use of Positron Emission based technology applied to breast cancer detection. In spite of initial very encouraging results in limited clinical trials, whole body PET systems have considerable operational costs, with a low patient turnover incompatible with systematic screening and a low spatial resolution which limits the minimum lesion size that can be detected. This has led to the development of dedicated PET scanners, targeting breast cancer imaging applications (Thompson et al, 1995, Moses, 2004). The PEM units are designed to explore localized regions of the body, usually the breast, and adopt several design principles, like fine pixelized crystals, to achieve a better spatial resolution, as well as a large count-rate capability. This set of requirements has lead to the development of a series of proof-of-principle and a few full-

assembled Positron Emission Mammography (PEM) scanner prototypes, several of which have been used in preliminary clinical trials, based on high density and high-Z inorganic scintillator crystals. Of this list, almost all lack the ability to measure the depth-of-interaction and thus reconstructed images may show significant aberrations due to the parallax effect. An emerging technique to reduce this aberration effect consists on the readout of the scintillation light, produced in the crystal elements, by two opposing photosensors and extracts the coordinate of interaction along the longitudinal axis from the asymmetry of light collection (Shao et al., 2000). This is particular important since in a planar detector with the active media located close to the object under examination, the parallax effect can be an important source of blurring in the spatial resolution.

Several technical challenges need to be addressed namely on how to readout the light from the crystals without putting unacceptable amounts of

non-active media (like conventional photomultipliers) between the patient port and the crystals, which would lead to a degradation on the final image quality and lesion detection sensitivity.

To address these issues, the Clear-PEM scanner (Lecoq and Varela, 2002, Abreu et al, 2006), was developed by the Portuguese PET Consortium, composed by: Laboratório de Instrumentação e Física Experimental de Partículas (LIP), Instituto de Biofísica e Engenharia Biomédica da Faculdade de Ciências de Universidade de Lisboa (IBEB), Instituto de Biomédico de Investigação de Luz e Imagem (IBILI), Instituto de Novas Tecnologias (INOV), Instituto de Engenharia de Sistemas e Computadores Investigação e Desenvolvimento (INESC-ID), Instituto de Engenharia Mecânica e Gestão Industrial (INEGI), Hospital Garcia da Orta (HGO), Instituto Português de Oncologia (IPO) in Porto and with the participation of CERN (Organisation Européenne pour la Recherche Nucléaire) through the international collaboration Crystal Clear Collaboration.

The detector is based on pixelized LYSO:Ce crystals optically coupled on both extremities to avalanche photodiodes (APD) and readout by a fast, low-noise electronic system. The choice of avalanche photodiodes was dictated by its compatibility with the implementation of a double readout technique. The APDs also demonstrate good energy resolution for a direct detection of X-rays and for LYSO:Ce scintillator light readout, with low multiplication noise and acceptable gain uniformity. The Hamamatsu S8550 APD was selected for the Clear-PEM detector, which offers a stable working regime up to gain 200 (Abreu et al., 2007), and has a dark current noise below 27 electrons ENC at room temperature (Kapusta et al., 2003).

The total number of APD arrays needed for a single scanner is 384, and the S8550 arrays were manufactured by Hamamatsu Photonics Inc. Japan. A total of 984 photodetectors were acquired for assessment.

A quality control protocol and methodology were developed in order to assess and characterize the acquired APDs. In this paper the adopted quality check procedures for the APD arrays is described and the controlled parameters are presented (gain dependence on bias voltage, gain variation at various voltages, dark current dependence on the bias voltage).

2 CLEAR-PEM IMAGING SYSTEM

2.1 Detector Heads

The Clear-PEM imaging system (Figure 1) is based on a two parallel detector heads design. The detector consists in two compact and planar detector heads with adequate dimensions for breast and axilla imaging. A dedicated gantry was built in order to allow the rotation of the detector heads in breast exams as well as to permit exams of the axilla region. Each detector head holds the scintillator material matrices and the frontend readout circuitry composed of multi-pixel APD photosensors, frontend ASIC chips, free-sampling ADCs and Channel Link LVDS serializers. Auxiliary sub-systems are also assembled in the detector heads, providing environmental monitoring, cooling, power supply and system clock distribution. A dedicated digital trigger and data acquisition system is used for online selection of coincidence events with high efficiency, large bandwidth and negligible dead-time (Albuquerque et al 2006, Albuquerque et al 2008a).

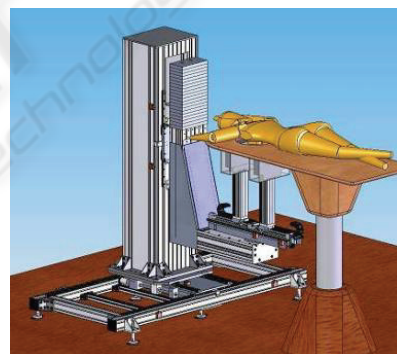


Figure 1: The Clear-PEM imaging system (CAD image).

The structure of a detector head starts in the detector module. The detector module is composed by the LYSO:Ce crystal matrix, optically coupled (through an optical glue) to a S8550 APD array, on each end, for DOI measurements. The APD array is mounted in a small PCB with a low footprint SMT connector on the back side. The components of the detector module are housed and sealed in a dedicated plastic assembly. The assembly has two empty slots in which two detector modules can be plug-in, defining a "double module". 12 detector modules are mechanically fixed and electrically connected to a front and back Frontend Boards (FEBs) forming a Supermodule (Figure 2) (Albuquerque et al, 2008b).

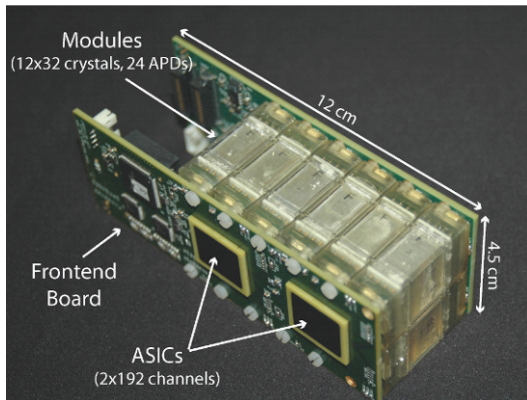


Figure 2: Supermodule structure assembling 12x32 LYSO:Ce crystals and 24 APDs in double readout. Each Frontend board has two 192 input channels ASICs.

The assembled modules underwent a quality control measurements carried out at LIP (Amaral et al., 2006). The electronics chips were mounted on the external faces of the two FEBs. Connectors for cables linking to the data acquisition system were also mounted in the PCBs. In a detector head, eight Supermodules, each with 12 modules, are mounted together.

The final prototype has two planar parallel detector heads with 192 detector modules, 6144 crystals and 384 APD arrays (12 288 APD pixels), covering a $17 \times 15 \text{ cm}^2$ Field-of-View.

2.1.1 Crystals

The chosen scintillator for the Clear-PEM was a inorganic crystal, LYSO:Ce. The LYSO:Ce is cerium activated lutetium–yttrium–ortho–silicate ($\text{Lu}_{2(1-x)}\text{Y}_{2x}\text{SiO}_5:\text{Ce}$) and has similar properties to LSO:Ce (Lu_2SiO_5) (Melcher and Schweitzer, 1992).

The choice of this scintillator was dictated by its high light output (27-30 photons/keV) compatible with good energy measurements (9% at 662 keV with a PMT readout), as well as a fast rise time and decay (42 ns time constant) compatible with high-quality timing measurements and low dead time. Its peak emission is short–blue/long ultraviolet (UV) wavelength (420 nm).

For the Clear-PEM scanner, crystals with dimensions of $2 \times 2 \times 20 \text{ mm}^3$ were chosen. The 20 mm longitudinal size guarantees a large detection efficiency for 511 keV photons and the determination of the DOI coordinate with a resolution of 2 mm (FWHM) (Abreu et al., 2006, Amaral et al., 2006).

In total the scanner uses 6144 pixel LYSO:Ce crystals (Figure 3a) divided in 192 matrices,

composed by a 4×8 LYSO:Ce crystal array (Figure 3b). In this configuration, the crystals are optically isolated by $300 \mu\text{m}$ BaSO_4 reflector walls. The BaSO_4 provide the crystal support and provides the diffuse reflecting surfaces needed to optimize the light collection and the DOI measurements.

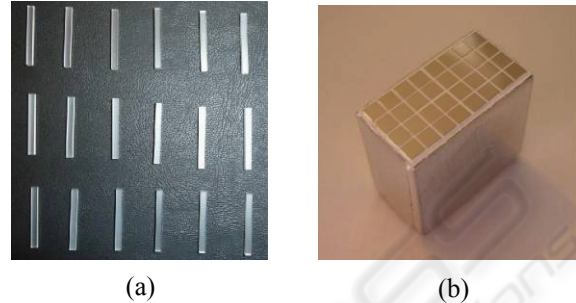


Figure 3: Photograph of (a) a sample of $2 \times 2 \times 20 \text{ mm}^3$ LYSO:Ce crystals produced for the Clear-PEM scanner and (b) an assembled BaSO_4 -type matrix.

2.1.2 Photosensors

The S8550 APD array from Hamamatsu Photonics with a 32 pixels in an 8×4 configuration was the selected photodetector for the Clear-PEM scanner (Figure 4a and b). The S8550 array is assembled from two distinct monolithic silicon wafer parts, of 2×8 "reverse" type structure pixel elements, and each 2×8 group is called an sub-array. The sub-array that contains the APD pixels from A1 to H1, and from A2 to H2, is called sub-array 1. The remaining pixels are contained in the sub-array 2. Each sub-array is biased independently. The pixels are mounted on a 1 mm thick ceramic package with a 0.5 mm thick epoxy window (Kapusta et al., 2003).

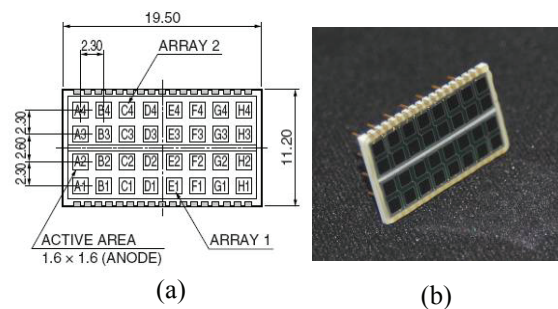


Figure 4: (a) Schematic representation of the 32 pixel Hamamatsu S8550 APD array (dimensions in millimetres) and (b) photograph of a S8550 APD array.

Each Si pixel element has a $1.6 \times 1.6 \text{ mm}^2$, compatible with an individual 1:1 readout of $2 \times 2 \text{ mm}^2$ cross-section LYSO:Ce crystals. The element pitch is 2.3 mm and all the pixels placed in the same sub-matrix share the same common bias.

A compilation of the Hamamatsu S8550 main electrical and optical characteristics are present in Table 1. The effective APD gain (ratio of the total number of secondary avalanche electrons produced by the initial number of electron-hole pairs due to the scintillation light) is between 70 and 350 with a specified inter-pixel gain variation less than 5% r.m.s. and a dark current of 2–4 nA per pixel. The terminal capacitance is 10 pF per pixel (Abreu et al., 2007).

Table 1: Hamamatsu S8550 APD 32 channel electrical and optical parameters (Abreu et al, 2007, Mosset, 2006).

Parameter	Hamamatsu S8550
Pixel Size	1.6 x 1.6 mm ²
Pixel Pitch	2.3 mm
Window Type	0.5 mm epoxy resin
Peak Wavelength	600 nm
QE @ 420 nm	72-76%
Gain (M)	50 – 350
Gain Gradient @ M=70	3.6%/V
Dark Current	2.4 nA (pixel @ M=70)
Capacitance	10 pF (pixel @ M=70)

The S8550 APD operates at a bias voltage of 360-500 V, depending on the required gain. The gain shows a temperature gradient of $-2.4\%/^{\circ}\text{C}$ at gain 70. This is due to lattice vibrations in the silicon structure of the APD which are enhanced as temperature increases making more probable to interact with avalanche secondary electrons. Temperature drifts, if not controlled, may thus originate gain drifts contributing to a deterioration of the energy resolution (Crespo et al., 2004, Spanoudaki et al., 2005). The temperature gradient is also function of the bias voltage, which means that at higher gains the APDs show an increased susceptibility to temperature drifts. All this imply that the system has to operate under stable thermal conditions. The gain gradient as function of the polarizing bias is observed to vary as function of the gain. For the highest gain the bias polarization supplies must be very stable with controlled amounts of tension ripple (Abreu et al., 2007).

2.2 Electronic Systems

The frontend and data acquisition electronics systems are key components in the developed PET system, enabling a high detection sensitivity and low random background noise, without compromising the spatial resolution, allowed by fine segmented crystals. The data acquisition and trigger electronics of the Clear-PEM scanner is composed by three main blocks (Albuquerque et al., 2006):

- The Frontend Electronics System, performs signal amplification, channel selection and analog multiplexing, analog to digital conversion and parallel-to-serial translation;
- The Trigger and Data Acquisition System, which implements the temporary data storage, first-level trigger (L1) computation and data transfer to the acquisition computer (DAE server);
- The Software Trigger (L2), implemented in the DAE server, in which the received data from the DAE crate is un-packed, extraction algorithms (time, energy, DOI) applied and the trigger re-validated;

The on-detector electronics includes the amplifier and analog multiplexing integrated circuits (frontend ASIC). The front-end system is based in a data-driven synchronous design that identifies and multiplexes the analog signals of channels above threshold, reducing the number of channels by a factor of 96. To transmit the signals from the detector heads, digital serializers are used to minimize the number of lines connecting to the trigger and data acquisition system (Rodrigues, 2007).

The off-detector system receives the serialized digitized data streams, applies a coincidence trigger based on the computation of the pulses amplitude and timing, and pushes the data into the data acquisition computer. The trigger and data acquisition logic is implemented in large FPGAs with 4 and 3 million gates respectively, with the trigger algorithm decomposed in a sequence of elementary operations executed in pipeline mode. The system was designed to operate at a maximum input clock frequency of 100 MHz and be able to sustain a data acquisition rate of 1 MHz with efficiency above 90–95%, under a maximum total single photon background rate in the detector of 10 MHz. The communication between the readout system and the data acquisition computer is established through a serial high-speed link allowing the off-detector crate to be located several meters away from the DAE server data acquisition computer.

2.3 Mechanical Systems

The Clear-PEM mechanical system was designed to allow the exam of both the breast and the auxiliary lymph nodes. The system is used in conjunction with a shielded examination table that enables exams to be performed with the patient kept in prone position. Configurable openings in the examination table

allow the exam of both breasts with the detector heads positioned in each side of the breast (Abreu et al., 2006). During the exam the detector heads can rotate around the detector main axis in order to collect data at several angular orientations as required for tomographic reconstruction.

The examinations of the breast region close to the chest and of the axilla region are performed in a front-back configuration. In these exams one detector head is facing the breast (complementary exam), or the shoulder (axilla exam), under the scanner table and the other is positioned against the patient back.

3 QUALITY CONTROL OF AVALANCHE PHOTODIODES

The scanner construction starts with the quality control (QC) and gain characterization of all APD arrays acquired by the PET consortium, in order to assess which ones are useable in the final prototype. The project commercially acquired 984 APD arrays which needed a fast evaluation. An automatic measuring setup was developed, based on the direct measurement of the APD-array common cathode current when illuminated by a blue LED light (to simulate the LYSO:Ce scintillation). This automatic measuring setup was named “APD Tester”. The blue light (420 nm) from the LED is homogeneously distributed by a light guide through all APD pixels.

The characterization consists in the measurement of the bias voltage needed to operate the APD arrays at gains 70, 150 and 350, the variation of gain per volt (dM/dV) at each of these gain regions, and also the Dark Current (I_d), for the same gain regions. Each individual APD sub-array is characterized independently (1968 sub-arrays, 9 characterization parameters each, gives a total of 17712 measurement values).

For the QC part, the chosen acceptance values at gain 70 were:

- Bias Voltage $\leq 500V$;
- Gain Variation $\leq 4.0\%/V$;
- Dark Current ≤ 160 nA (10 nA per pixel);

The parameters were selected accordingly to the Hamamatsu specifications (and tolerances) and are applied to each sub-array. If one of the parameters is not approved, the APD array is marked as “bad” and sent back to the manufacturer.

3.1 APD Tester

The APD Tester is a dedicated electronic setup for the Hamamatsu APD array S8550 gain and dark Current quality control and characterization (Figure 5). One of the main features of this dedicated electronic system is the automatization of the measurement procedure, in order to save time and manpower. It measures 16 APD arrays (32 sub-arrays) in a single run (or several), in about 4 hours. It also controls the blue LED, used to simulate the scintillation light.

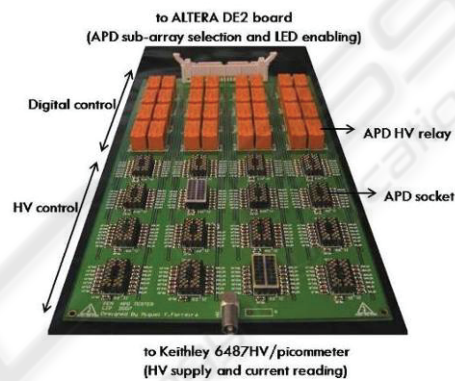


Figure 5: APD Tester, an electronic setup designed to the automatic characterization of the S8550 APD Array.

The electronic was completely designed and developed at LIP. The Tester was assembled inside a metal box (Faraday cage) due to the need of a protection from any outside signal interference, and to keep the APD arrays away from the outside light. The LED is located inside the box and is coupled to a light guide to provide an equal light distribution to all APD sub-arrays (and pixels). The tester setup is composed by two major parts: HV Control and Digital Control.

The digital control is composed by HV relays to select the APD sub-array to be measured, from the possible 32. The relays are controlled through a FPGA Cyclone II (ALTERA DE2 Board) via serial port. The LED is also controlled by the digital part.

The HV Control receives the HV from a Keithley 6487 Picometer/Voltage Source, controlled via serial port, and delivers it to the enabled APD sub-array. The automatic setup, and the Keithley, are controlled via serial ports by a LabView program, which selects the measurement type and collects the data into an excel file.

3.2 Experimental Setup

The experimental setup is composed by the APD Tester (in the Faraday cage), a Keithley 6487 Picoammeter / Voltage Source and a PC. The gain calculation assumes that when the APD sub-array is biased at 30V (with the LED on), the gain is 1. From that value the M=70, 150 and 350 are calculated. For the dark current measurements the LED is turned off and the residual current is measured. The schematic of the experimental setup can be found in Figure 6.

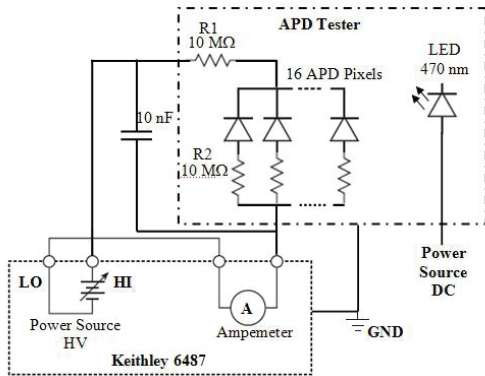


Figure 6: Schematic representation of the experimental setup for gain and dark current measurements.

3.3 Measurement Procedure

Each measurement run is accompanied by a stability check procedure (performance on a reference APD array) in order to evaluate the setup in terms of significant variations on the studied parameters. The setup operates at a stable temperature (through AC control) of approximately 24°C, in order to minimize temperature dependence deviations. The complete measurement took about 30 working days (2 run sets per day approximately). The stability check consists in the measurement of a predefined APD array, the control APD. Each measurement run characterized 15 new APD plus the control APD.

3.3.1 Bias Voltage Quality Control and Characterization

The 984 APD matrices (1968 sub-arrays) were characterized in bias voltage terms and Table 2 summarizes the results.

All APD passed the HV QC at M=70 (the bias voltage values were all below 500V) -

Figure 7. The HV values oscillated between 360 and 459 V - Figure 8.

Table 2: Bias Voltage average values for gains M=70, 150 and 350 from the 984 APD arrays (also the maximum and minimum HV).

	Bias Voltage (V)	Sub-array 1	Sub-array 2
M=70	Average (r.m.s)	419 ± 22	418 ± 21
	Minimum	360	364
	Maximum	458	459
M=150	Average (r.m.s)	434 ± 22	434 ± 21
	Minimum	375	379
	Maximum	473	474
M=350	Average (r.m.s)	443 ± 22	442 ± 21
	Minimum	384	389
	Maximum	482	481

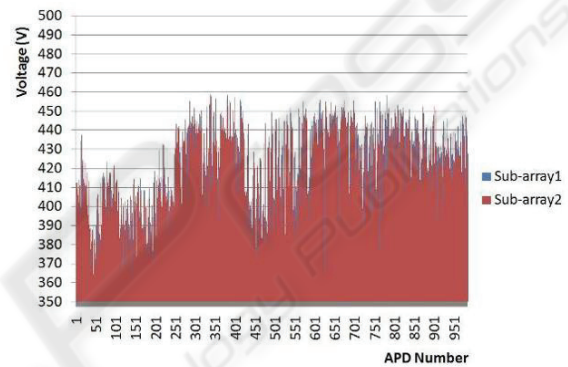


Figure 7: High Voltage per APD sub-array distribution at M=70.

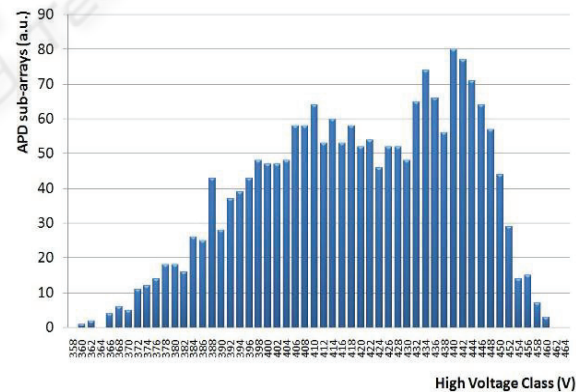


Figure 8: High Voltage histogram for M=70 values.

3.3.2 Gain Variation Quality Control and Characterization

The gain variation of the 984 APD matrices was characterized and Table 3 summarizes the results.

All but one APD sub-array had a gain variation of less than 4%/V, passing the Gain variation quality control at M=70 – Figure 9.

The APD that didn't pass the QC procedure had a dM/dV of about 22.7 % on the second sub-array (the other had a normal value, 3.2 %/V).

Table 3: Gain Variation average values for gains M=70, 150 and 350 from the 984 APD arrays (also the maximum and minimum dM/dV).

	Gain Variation (%/V)	Sub-array 1	Sub-array 2
M=70	Average (r.m.s)	3.6 ± 0.1	3.6 ± 0.6
	Minimum	3.2	3.3
	Maximum	4.0	22.7
M=150	Average (r.m.s)	6.3 ± 1.8	6.0 ± 0.8
	Minimum	5.4	5.4
	Maximum	26.5	19.4
M=350	Average (r.m.s)	14.0 ± 4.7	13.5 ± 4.6
	Minimum	9.2	6.0
	Maximum	30.7	31.6

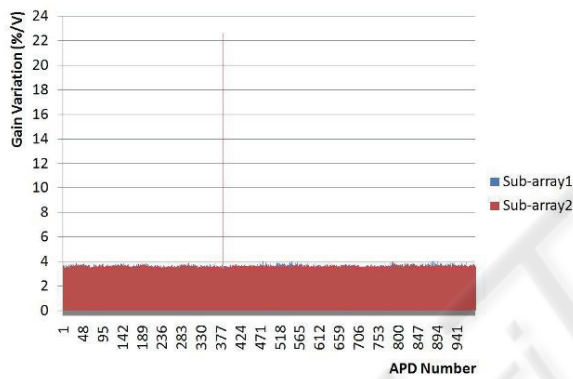


Figure 9: Gain Variation per APD sub-array distribution at M=70.

3.3.3 Dark Current Quality Control and Characterization

The Dark Current characterization of the 984 APD matrices was completed and Table 4 summarizes the results.

All APD sub-array passed the Dark Current QC at M=70 (all the values were below the stipulated maximum limit of 160nA, less than 10 nA per APD pixel according to Hamamatsu Photonics) – Figure 10.

4 CONCLUSIONS

The quality control and characterization procedure for the acquired APD arrays for the Clear-PEM prototype was defined and implemented. A dedicated automatic APD characterization

electronics was developed and built. The 984 Hamamatsu S8550 APD arrays were submitted to the QC and characterization procedure at gains 70, 150 and 350, in terms of bias voltage, dark current and gain variation per volt.

Table 4: Dark Current average values for gains M=70, 150 and 350 from the 984 APD arrays (also the maximum and minimum Id).

	Dark Current (nA)	Sub-array 1	Sub-array 2
M=70	Average (r.m.s)	27.1 ± 13.3	24.2 ± 10.1
	Minimum	7.8	8.2
	Maximum	88.9	67.6
M=150	Average (r.m.s)	43.1 ± 21.1	40.0 ± 19.2
	Minimum	10.1	12.1
	Maximum	138.4	300.0
M=350	Average (r.m.s)	107.1 ± 67.0	103.7 ± 65.9
	Minimum	15.9	17.6
	Maximum	334.2	700.0

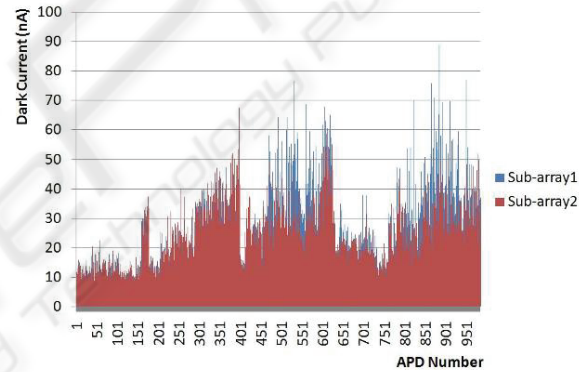


Figure 10: Dark Current per APD sub-array distribution at M=70.

The QC (M=70) had very good results: average bias voltage of 419 and 418V for sub-array1 and 2 respectively, average dark current of 27.1 and 24.2nA, for sub-array1 and 2, and average gain variation of 3.6%/V for both sub-arrays.

From a total of 984 tested APD arrays only 1 (0.1%) didn't pass the QC procedure (due to a 22.7%/V gain variation in the second sub-array). The small variance on the different electrical characterization parameters points out that current available APDs are suitable for high-integration PET prototypes which could not be implemented using a classical photomultiplier readout.

ACKNOWLEDGEMENTS

The authors would like to thank colleagues from the Portuguese PET Consortium and the Crystal Clear Collaboration for their suggestions and contribution. This project is financed by AdI (Agência de Inovação) and POSI (Operational Program for Information Society), Portugal. The work of P. Rodrigues and A. Trindade was supported by FCT under grants SFRH/BPD/37233/2007 and SFRH/BPD/37226/2007. The work of R. Bugalho, B. Carriço, C. S. Ferreira, R. Moura, C. Ortigão and J. F. Pinheiro was supported by AdI.

REFERENCES

- Abreu, M. C., Aguiar, J. D., Almeida, F. G., Almeida, P., Bento, P., Carriço, B., Ferreira, M., Ferreira, N. C., Gonçalves, F., Leong, C., Lopes, F., Lousã, P., Martins, M. V., Matela, N., Mendes, P. R., Moura, R., Nobre, J., Oliveira, N., Ortigão, C., Peralta, L., Pereira, R., Rego, J., Ribeiro, R., Rodrigues, P., Sampaio, J., Santos, A. I., Silva, L., Silva, J. C., Sousa, P., Teixeira, I. C., Teixeira, J. P., Trindade, A., and Varela, J. (2006). *Design and evaluation of the Clear-PEM scanner for positron emission mammography*. IEEE Trans. Nuc. Sci., 53:71–77.
- Abreu, M. C., Amaral, P., Carriço, B., Ferreira, M., Moura, R., Ortigão, C., Rato, P., and Varela, J. (2007). *Characterization and quality control of avalanche PhotoDiode arrays for the Clear-PEM detector modules*. Nucl. Instr. and Method., 576(1):19–22.
- Albuquerque, A., V. Bexiga, Bugalho, R., Carriço, B., Ferreira, C. S., Ferreira, M., Godinho, J. Gonçalves, F., Leong, C., Lousã, P., Machado, P., Moura, R., Neves, P., Ortigão, C., Piedade, F., Pinheiro, J. F., Rivetti, A., Rodrigues, P., Silva, J. C., Silva, M. M., Teixeira, I. C., Teixeira, J. P., Trindade, A., Varela, J. (2008) *Experimental characterization of the 192 channel Clear-PEM frontend ASIC for multi-pixel APD readout*. Sub. Nucl. Instr. And Method.
- Albuquerque, E., Almeida, F. G., Almeida, P., Augusto, S., Bexiga, V., Bugalho, R. Carmona, S., Carriço, B., Ferreira, C. S., Ferreira, N. C., Ferreira, M., Godinho, J., Gonçalves, F., Guerreiro, C., Leong, C., Lousã, P., Machado, P., Martins, M. V., Matela, N., Moura, R., Neves, P., Oliveira, N., Ortigão, C., Piedade, F., Pinheiro, J. F., Rego, J., Relvas, P., Rivetti, A., Rodrigues, P., Sá, D. N., Sampaio, J., Santos, A. I., Silva, M. M., Teixeira, I. C., Teixeira, J. P., Silva, J. C., Trindade, A., Varela, J. *Performance evaluation of a highly integrated APD/ASIC double-readout supermodule with 768 channels for Clear-PEM*, In 2008 IEEE Nuclear Science Symposium Conference Record.
- Amaral, P., Carriço, B., Ferreira, M., Moura, R., Ortigão, C., Rodrigues, P., Silva, J. C., Trindade, A., and Varela, J. (2006). *Performance and quality control of Clear-PEM detector modules*. Nucl. Instr. and Method. in press.
- Albuquerque, E., Bento, P., Leong, C., Gonçalves, F., Nobre, J., Rego, J., Relvas, P., Lousã, P., Rodrigues, P., Teixeira, I. C., Teixeira, J. P., Silva, L., Silva, M. M., Trindade, A., and Varela, J. (2006). *The Clear-PEM electronics system*. IEEE Trans. Nuc. Sci., 53(5):2704–2711.
- Crespo, P., Kapusta, M., Pawelke, J., Moszyński, M., and Enghardt, W. (2004). *First in-beam PET imaging with LSO/APD array detectors*. IEEE Trans. Nuc. Sci., 51(5):2654–2661.
- Kapusta, M., Crespo, P., Wolski, D., Moszyński, M., and Enghardt, W. (2003). *Hamamatsu S8550 arrays for high-resolution scintillator matrices readout*. Nucl. Instr. and Method., A504:139–142.
- P. Lecoq and J. Varela, *Clear-PEM, a dedicated PET camera for mammography*. Nucl. Instrum. Meth. vol A 486, pp.1-6, 2002.
- Melcher, C. L. and Schweitzer, J. S. (1992). *Cerium-doped lutetium oxyorthosilicate: a fast, efficient new scintillator*. IEEE Trans. Nuc. Sci., 39(4):502–505.
- Moses, W. W. (2004). *Positron emission mammography imaging*. Nucl. Instr. and Method., A525(1–2).
- Mosset, J. B. (2006). *Developpement d'un module de detection phoswich LSO%LuYAP pour le prototype de camera a positrons ClearPET*. PhD thesis, Faculte des Sciences de base de l'Ecole Polytechnique Federale de Lausanne.
- Rodrigues, P., (2007). *Study and Development of the Clear-PEM Trigger and Data Acquisition System ClearPET*. PhD thesis, Instituto Superior Técnico, Universidade Técnica de Lisboa.
- Spanoudaki, V., McElroy, D. P., Zell, K., and Ziegler, S. I. (2005). *Effect of temperature on the stability and performance of an LSO-APD PET scanner*. In 2005 IEEE Nuclear Science Symposium Conference Record, pages 2785–2789.
- Shao, Y., Silverman, R. W., Farrell, R., Cirignamo, L., Grazioso, R., Shah, K. S., Visser, G., Clajus, M., Tumer, T. O., and Cherry, S. R. (2000). *Design studies of a high resolution PET detector using APD arrays*. IEEE Trans. Nuc. Sci., 47(3):1051–1057.
- Thompson, C. J., Murthy, K., Picard, Y., Weinberg, I. N., Mako F. M. (1995) *Positron Emission Mammography (PEM): a promising technique to detect breast cancer*. IEEE Trans. Nucl. Sci. 42 1012–1017.